

Transverse vibration analysis of rotating porous beam with functionally graded microstructure using the differential transform method

Farzad Ebrahimi · Mohadese Mokhtari

Received: 26 July 2014 / Accepted: 26 September 2014 / Published online: 10 October 2014
© The Brazilian Society of Mechanical Sciences and Engineering 2014

Abstract This study presents free vibration analysis of rotating functionally graded Timoshenko beam made of porous material using the semi-analytical differential transform method. The material properties are supposed to vary along the thickness direction of the beam according to the rule of mixture, which is modified to approximate the material properties with the porosity phases. The frequency equation is obtained using Hamilton's principle. It is demonstrated that the DTM has high precision and computational efficiency in the vibration analysis of porous FG rotating beams. The good agreement between the results of this article and those available in literature validated the presented approach. Detailed mathematical derivations are presented and numerical investigations are performed, while emphasis is placed on investigating the effect of the several parameters such as porosity, functionally graded microstructure, thickness ratio, rotational speed and hub radius on the normalized natural frequencies of porous FG rotating beams in detail.

Keywords Porous material · Functionally graded material · Rotating beam · Differential transform method

1 Introduction

In an effort to develop super heat-resistant materials, Japanese material scientists proposed the concept

of FGM in the early 1980s. These materials, which are microscopically heterogeneous and are typically made from isotropic components, such as metals and ceramics, were initially designed as thermal barrier materials for aerospace structures and fusion reactors [3]. FGMs are composite materials with inhomogeneous micromechanical structure and are generally composed of two different parts such as ceramic and metal, in which the material properties change smoothly between two surfaces. This kind of material as a novel generation of composites of microscopical heterogeneity is achieved by controlling the volume fractions, microstructure, porosity, etc. of the material constituents during manufacturing, resulting in spatial gradient of macroscopic material properties of mechanical strength and thermal conductivity. As a result, in comparison with traditional composites, FGMs possess various advantages, for instance, ensuring smooth transition of stress distributions, minimization or elimination of stress concentration, and increased bonding strength along the interface of two dissimilar materials. Therefore, FGMs have received wide applications in modern industries including aerospace, mechanical, electronics, optics, chemical, biomedical, nuclear, and civil engineering to name a few during the past two decades. Moreover, porous FGMs have some other specific applications, as thermal barrier coatings and filtration and also in biomaterial usages such as dental implants and bone replacements. Motivated by these engineering applications, FGMs have also attracted intensive research interests, which were mainly focused on their static, dynamic, and vibration characteristics of FG structures [4, 5]. Rotating FG beams attached to a rigid hub occur in different engineering applications such as wind turbines, gas turbines, ship propellers, helicopter rotor blades, robot manipulators, and spinning space structures. To

Technical Editor: Fernando Alves Rochinha.

F. Ebrahimi (✉) · M. Mokhtari
Department of Mechanical Engineering, Faculty of Engineering,
Imam Khomeini International University, P.O.B. 16818-34149,
Qazvin, Iran
e-mail: febrahimi@eng.ikiu.ac.ir

control the vibration behavior of these bodies it is important to find natural frequencies.

Further, the increasing use of beams as structural components in various fields such as marine, civil, and aerospace engineering has necessitated the study of their vibration behavior and a large number of studies can be found in literature about transverse vibration of uniform isotropic beams. In this study, a relatively new approach called differential transformation method (DTM) is applied in analyzing vibration analysis of rotating FG beams. The concept of DTM was first proposed by Zhou [12] in solving linear and non-linear initial value problems in electrical circuit analysis. The superiority of the DTM is its simplicity and good precision and depends on Taylor series expansion, while it takes less time to solve polynomial series. It is different from the traditional high-order Taylor's series method, which requires symbolic competition of the necessary derivatives of the data functions. The Taylor series method computationally takes a long time for large orders. With this method, it is possible to obtain highly accurate results or exact solutions for differential equations. With this technique, the given partial differential equation and related initial conditions are transformed into a recurrence equation that finally leads to the solution of a system of algebraic equations as coefficients of a power series solution. This method is useful for obtaining exact and approximate solutions for both linear and nonlinear ordinary and partial differential equations, and there is no need for linearization or perturbations, and large computational work and round-off errors are avoided. It is a proper method to analyze beam vibrations. A study on rotating Timoshenko beams by differential transform method has been presented by some researchers [6, 8].

Due to porosities occurring inside FGMs during fabrication, it is therefore necessary to consider the vibration behavior of beams having porosities in this investigation. The porous materials are composed of two elements, one of which is solid (body) and the other element is either liquid or gas that is frequently found in nature, such as wood, stone, and layers of dust. For many years, porous material structures, such as beams, plates, and shells, have been widely discussed in structural design problems. The problem of vibration of the porous structures has been studied by some authors. For example, Wattanasakulpong et al. [11] analyzed free vibration of layered functionally graded beams and validated their results with experimental results; they concluded that discrepancies between theoretical and experimental results could arise from porosities due to imperfect infiltration and from approximation in material profile in calculation. Wattanasakulpong and Ungbhakorn [10] studied linear and nonlinear vibration analysis of elastically restrained end FGM beams. They used a modified form of rule of mixture to describe the material properties

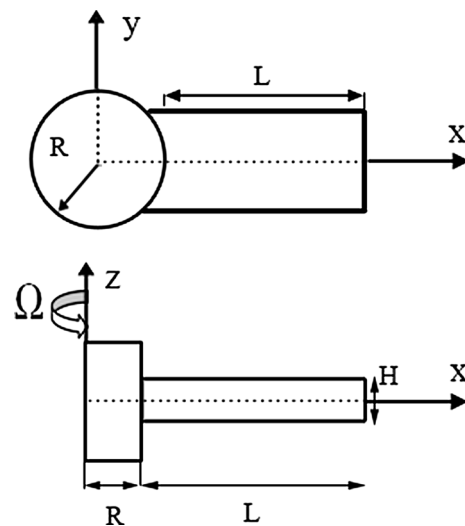


Fig. 1 Typical functionally graded beam with Cartesian coordinates

of the FG beam with porosities. But in all of these articles, the FG beam is not rotating and thus the need for investigation of vibration characteristics of the rotating porous FG beams is very much felt, but it has not been found in the literature. Consequently, in this study, the semi-analytical DTM method is applied for studying the vibration characteristics of rotating thick porous FG beam considering the effects of shear deformation and rotatory inertia within the context of Timoshenko beam theory. The gradation of material properties is assumed to be along the thickness of the beam. Comparisons with the results from the existing literature are provided for validation in special cases. Numerical results are presented to examine the effect of several beam parameters such as constituent volume fractions, slenderness ratios, rotational speed, and hub radius on vibration behavior of the rotating porous FG beam.

2 Theory and formulation

2.1 Functionally graded porous material

One of the most favorable models for FGMs is the power-law model, in which the material properties of FGMs are assumed to vary according to a power law about spatial coordinates. The coordinate system for FGM rotating beam is shown in Fig. 1. The length of the beam is L and thickness is h . The FG beam is attached to the periphery of a rigid hub of radius R and the hub rotates about the z -axis at a constant angular speed Ω . A Cartesian coordinate system $O(x, y, z)$ is defined on the central axis of the beam where the x axis is taken along the central axis, the y -axis in the

width direction, and the z -axis in the depth direction. The FG beam is assumed to be composed of ceramic and metal, and the effective material properties (P_f) of the FG beam such as Young’s modulus E_f , shear modulus G_f and mass density ρ_f are assumed to vary continuously in the thickness direction (z -axis direction) according to a power function of the volume fractions of the constituents, while the Poisson’s ratio is assumed to be constant in the thickness direction.

V_m and V_c are the material properties and the volume fractions of the metal and the ceramic constituents related by:

$$V_c + V_m = 1. \tag{1a}$$

The volume fraction of the metal constituent of the beam is assumed to be given by:

$$V_c = \left(\frac{z}{h} + \frac{1}{2}\right)^P \tag{1b}$$

Here, P is the non-negative variable parameter (power-law exponent) which determines the material distribution through the thickness of the beam. The modified rule of mixture to find the effective material properties of porous beam (P) can be expressed as follows [10]

$$P_f(z) = (P_c - P_m)\left(\frac{z}{h} + \frac{1}{2}\right)^k + P_m - (P_c + P_m)\frac{\alpha}{2} \quad \alpha \ll 1 \tag{2}$$

$$E_f(z) = (E_c - E_m)\left(\frac{z}{h} + \frac{1}{2}\right)^k + E_m - (E_c + E_m)\frac{\alpha}{2} \tag{3}$$

$$\rho_f(z) = (\rho_c - \rho_m)\left(\frac{z}{h} + \frac{1}{2}\right)^k + \rho_m - (\rho_c + \rho_m)\frac{\alpha}{2}. \tag{4}$$

Here, α is the volume fraction of porosity. According to this distribution, the bottom surface ($z = -h/2$) of functionally graded beam is pure metal, whereas the top surface ($z = h/2$) is pure ceramics.

2.2 Formulation of porous FGM beam using Timoshenko beam theory

In a Cartesian coordinate system, x is the distance of the point from the hub edge parallel to the beam length, u_0 is the axial displacement due to the centrifugal force, z is the vertical distance of the point from the middle plane, w is the transverse displacement of any point on the neutral axis, and θ is the rotation due to bending. Displacement field components are considered based on Timoshenko

beam theory. Considering [7] assumption and neglecting terms which are greater than ε_2 , the strain–displacement and strain energy simplified relations are calculated as follows:

$$\varepsilon_{xx} = u'_0 - z\theta' + \frac{(w')^2}{2} \tag{5}$$

$$\gamma_{xz} = w' - \theta \tag{6}$$

$$\gamma_{xy} = 0. \tag{7}$$

Bending strain energy U_b and shear strain energy U_s are given, respectively, by:

$$U_b = \int \int \int_V \frac{E(z)\varepsilon^2}{2} dV \tag{8}$$

$$U_s = \int \int \int_V \frac{G(z)\gamma^2}{2} dV. \tag{9}$$

Substituting Eqs. (5–7) into Eqs. (8–9) leads to

$$U_b = \frac{1}{2} \int_A \int_0^L E(z) \left\{ u'_0 - z\theta' + \frac{(w')^2}{2} \right\}^2 dA dx \tag{10}$$

$$U_s = \int \int \int_V \frac{G(z)(\gamma_{xy}^2 + \gamma_{xz}^2)}{2} dV. \tag{11}$$

Further, the total strain energy is given by:

$$U = U_s + U_b \infty. \tag{12}$$

Here, A_1 and A_2 are bending rigidity and axial rigidity of the beam cross section, respectively, and are defined as:

$$(A_1, A_2) = \int_{-h/2}^{h/2} E(z)(1, z^2) dA. \tag{13}$$

B_1 and B_2 are normal and rotary inertia terms, respectively, and C is the shear rigidity factor which are as follows:

$$(B_1, B_2) = \int_{-h/2}^{h/2} \rho(z)(1, z^2) dA \tag{14}$$

$$C = \int kG(z) dA, \tag{15}$$

where A , ρ , and E are the area of cross section, the mass density, and modulus of elasticity of the beam, respectively; G is the shear modulus and k is the Timoshenko shear correction factor which has been assumed equal to the isotropic case, i.e., $k = 5/6$. The axial displacement

$u'_0(x)$, which is uniform across the cross section, is related to strain $\varepsilon_0(x)$ by:

$$u'_0(x) = \varepsilon_0(x) = \frac{T(x)}{A_1}. \tag{16}$$

The centrifugal force $T(x)$ is defined as:

$$T(x) = \int_x^L B_1 \Omega^2 (R + x) dx. \tag{17}$$

According to Eqs. (13–17) bending and shear strain energy are obtained, respectively, as follows:

$$U_b = \frac{1}{2} \int_0^L (A_2(\theta')^2 + T(w')^2) dx + \text{const} \tag{18}$$

$$U_s = \frac{1}{2} \int_0^L C(w' - \theta) dx. \tag{19}$$

Further, substituting Eqs. (18–19) into Eq. (12) one gets the total strain energy of the beam in the following form:

$$U = \frac{1}{2} \int_0^L A_2(\theta')^2 + T(w')^2 + C(w' - \theta) dx. \tag{20}$$

Also the kinetic energy expression is given as:

$$\tau = \frac{1}{2} \int_A \int_0^L (V_x^2 + V_y^2 + V_z^2) \rho \, dA \, dx \tag{21}$$

The total velocity \vec{V} can be expressed in terms of deformed positions as:

$$\vec{V} = (\dot{x}_1 - \Omega y_1) \vec{i} + (\dot{y}_1 + \Omega x_1) \vec{j} + \dot{z}_1 \vec{k} \tag{22}$$

$$V_x = -\xi \dot{\theta} - \eta \Omega \tag{23}$$

$$V_y = (R + x + u_0 - \xi \theta) \Omega \tag{24}$$

$$V_z = \dot{w}. \tag{25}$$

Now, substituting Eqs. (22–24) into Eq. (20) kinetic energy is obtained as follows:

$$\tau = \frac{1}{2} \int_0^L [B_1 \dot{w}^2 + A_2 \dot{\theta}^2 + A_2 \Omega^2 \theta^2] dx. \tag{26}$$

2.3 Deriving governing equations for rotating FG beam

Hamilton’s principle is used herein to derive the equations of motion. The principle can be stated in analytical form as:

$$\int_{t_1}^{t_2} (\delta U + \delta V - \delta \tau) = 0, \tag{27}$$

where t_1 and t_2 are the initial and end time, respectively; δU is the virtual variation of the strain energy; δV is the virtual variation of the potential energy; and $\delta \tau$ is the virtual variation of the kinetic energy. According

to Hamilton’s principle, the equations of motion can be obtained as:

$$-B_2 \ddot{\theta} + B_2 \Omega^2 \theta + A_2 \theta'' + kC(W' - \theta) = 0 \tag{28}$$

$$-B_1 \ddot{W} + (TW')' + kC(W'' - \theta') = 0. \tag{29}$$

Further, the two ends of the Timoshenko cantilever beam ($x = 0$ and $x = L$) are subjected to the following boundary conditions:

$$\text{at } x = 0 : \quad W(0) = 0, \theta(0) = 0 \tag{30}$$

$$\text{at } x = L : \quad \theta'(L) = 0, W'(L) - \theta(L) = 0. \tag{31}$$

Assuming simple harmonic oscillation, w and θ can be written as:

$$W(x, t) = \bar{W}(x) e^{i\omega t} \tag{32}$$

$$\theta(x, t) = \bar{\theta}(x) e^{i\omega t}. \tag{33}$$

Substituting Eqs. (32) and (33) into Eqs. (28) and (29), the governing equations are as follows:

$$B_2 \omega^2 \bar{\theta} + B_2 \Omega^2 \bar{\theta} + A_2 \bar{\theta}'' + A_2 \bar{\theta}'' + kC(\bar{W}' - \bar{\theta}) = 0 \tag{34}$$

$$B_1 \omega^2 \bar{W} + (T\bar{W}')' + kC(\bar{W}'' - \bar{\theta}') = 0. \tag{35}$$

The dimensionless parameters which were found according to FGM characteristics are used to simplify the equations and to make comparisons with the studies in literature such as that by Banerjee [2]. These are given as follows:

$$\eta^2 = \frac{B_1 L^4 \Omega^2}{A_2}, \quad r^2 = \frac{B_2}{A_1 L^2}, \quad \delta = \frac{R}{L}, \quad \xi = \frac{x}{L}, \quad W(\xi) = \frac{\bar{W}}{L}$$

$$\mu^2 = \frac{B_1 L^4 \omega^2}{A_2}, \quad s^2 = \frac{A_2}{kCL^2}. \tag{36}$$

Then dimensionless expressions for centrifugal force and governing equations are obtained as follows:

$$T(\xi) = B_1 \Omega^2 L^2 \left[\delta(1 - \xi) + \frac{(1 - \xi^2)}{2} \right] \tag{37}$$

$$\bar{\theta}'' + \eta^2 r^2 \left(1 + \frac{\omega^2}{\Omega^2} \right) \bar{\theta} + \frac{1}{s^2} (\bar{W}' - \bar{\theta}) = 0. \tag{38}$$

$$\left\{ \left[\delta(1 - \xi) + \frac{(1 - \xi^2)}{2} \right] \bar{W}' \right\}' + \left(\frac{\omega^2}{\Omega^2} \right) \bar{W} + \frac{1}{s^2 \eta^2} (\bar{W}'' - \bar{\theta}') = 0. \tag{39}$$

Table 1 Some of the transformation rules of the one-dimensional DTM

Original function	Transformed function
$y(x) = \lambda\varphi(x)$	$Y(k) = \lambda\Phi(k)$
$y(x) = \varphi(x) \pm \theta(x)$	$Y(k) = \Phi(k) \pm \Theta(k)$
$y(x) = \frac{d\varphi}{dx}$	$Y(k) = (k + 1)\Phi(k + 1)$
$y(x) = \frac{d^2\varphi}{dx^2}$	$Y(k) = (k + 1)(k + 2)\Phi(k + 1)$
$y(x) = \varphi(x)\theta(x)$	$Y(k) = \sum_{l=0}^k \Phi(l)\Theta(k - l)$
$y(x) = x^m$	$Y(k) = \delta(k - m) = \begin{cases} 1 & k = m \\ 0 & k \neq 0 \end{cases}$

Table 2 Transformed boundary conditions (B.C.) based on DTM

X = 0		X = 1	
Original BC	Transformed BC	Original BC	Transformed BC
$f(0)$	$F[0] = 0$	$f(1)$	$\sum_{k=0}^{\infty} F[k] = 0$
$\frac{df}{dx}(0) = 0$	$F[1] = 0$	$\frac{df}{dx}(1) = 0$	$\sum_{k=0}^{\infty} kF[k] = 0$
$\frac{d^2f}{dx^2}(0) = 0$	$F[2] = 0$	$\frac{d^2f}{dx^2}(1) = 0$	$\sum_{k=0}^{\infty} k(k - 1)F[k] = 0$
$\frac{d^3f}{dx^3}(0) = 0$	$F[3] = 0$	$\frac{d^3f}{dx^3}(1) = 0$	$\sum_{k=0}^{\infty} k(k - 1)(k - 2)F[k] = 0$

2.4 Implementation of differential transform method

Generally, it is rather difficult to derive an analytical solution for Eqs. (38–39) due to the nature of non-homogeneity. In this circumstance, the DTM is employed to translate Eqs. (34–35) into a set of ordinary equations. First, the procedure of differential transform method is briefly reviewed. Differential transformation of function $y(x)$ according to [1] is defined as follows:

$$Y(k) = \frac{1}{k!} \left[\frac{d^k}{dx^k} y(x) \right]_{x=0}, \tag{40}$$

in which $y(x)$ is the original function and $Y(k)$ is the transformed function. Also, the differential inverse transformation of $Y(k)$ can be obtained as follows:

$$y(x) = \sum_{n+1}^{\infty} x^k Y(k). \tag{41}$$

Consequently from Eqs. (40–41), we obtain:

$$y(x) = \sum_{k=0}^n \frac{x^k}{k!} \left[\frac{d^k}{dx^k} y(x) \right]_{x=0}. \tag{42}$$

Equation (42) reveals that the concept of the differential transformation is derived from Taylor’s series expansion. In real applications, the function $y(x)$ in Eq. (41) can be written in a finite form as:

$$y(x) = \sum_{k=0}^n x^k Y(k). \tag{43}$$

In these calculations $y(x) = \sum_{n+1}^{\infty} x^k Y(k)$ is small enough to be neglected, and n is determined by the convergence of the eigenvalues. In Table 1, the basic theorem of DTM is stated, while Table 2 presents the differential transformation of conventional boundary conditions. Applying the DTM rule on the equations of motion (38–39) and boundary conditions (30–31), the next four equations are obtained as:

$$\begin{aligned} & \left(\delta + 0.5 + \frac{1}{s^2\eta^2} \right) (k + 1)(k + 2)W(k + 2) \\ & - \delta(k + 1)^2W(k + 1) + \left(\frac{\omega^2}{\Omega^2} - \frac{k(k + 1)}{2} \right) W(k) \\ & - \frac{1}{s^2\eta^2} (k + 1)\theta(k + 1) = 0 \end{aligned} \tag{44}$$

$$\begin{aligned} & (k + 1)(k + 2)\theta(k + 2) + \left[\eta^2 r^2 \left(1 + \frac{\omega^2}{\Omega^2} \right) - \frac{1}{s^2} \right] \theta(k) \\ & + \frac{1}{s^2} (k + 1)W(k + 1) = 0 \end{aligned} \tag{45}$$

$$\sum_{i=0}^n k * \Theta(k) = 0 \tag{46}$$

$$\sum_{i=0}^n k * w(k) - \Theta(k) = 0, \tag{47}$$

where $W(k)$ and $\theta(k)$ are the differential transforms of $w(\xi)$ and $\theta(\xi)$, respectively. Substituting $W(k)$ and $\theta(k)$ in Eqs. (46–47), we have:

$$M_{j1}^{(n)} c_1 + M_{j2}^{(n)} c_2 = 0, \quad j = 1, 2, 3, \dots, n, \tag{48}$$

in which M_{ij} are polynomials in terms of ω corresponding to the n th term. The matrix form of Eq. (48) can be prescribed as:

$$\begin{bmatrix} M_{11}^{(n)} & M_{12}^{(n)} \\ M_{21}^{(n)} & M_{22}^{(n)} \end{bmatrix} \begin{Bmatrix} c_1 \\ c_2 \end{Bmatrix} = 0. \tag{49}$$

Further, studying the existence condition of the non-trivial solutions yields the following characteristic determinant:

$$\begin{vmatrix} M_{11}^{(n)} & M_{12}^{(n)} \\ M_{21}^{(n)} & M_{22}^{(n)} \end{vmatrix} = 0. \tag{50}$$

Solving Eq. (50), the i th estimated eigenvalue for the n th iteration ($\omega = \omega_i^{(n)}$) may be obtained and the total number of iterations is related to the accuracy of calculations which can be determined by the following equation:

Table 3 Material properties of the FGM constituents [9]

Properties	Unit	Aluminum	Alumina (Al ₂ O ₃)
E	Gpa	70	80
ρ	kg/m ³	2,702	3,960
ν	–	0.3	0.3

Table 4 Convergence study of the first three frequencies, $L/h = 20$, $P = 2$, and $\eta = 4$

Iteration	λ_1	λ_2	λ_3
19	31.5639		
20	31.5781	135.4764	
21	31.5287	135.5118	
22	31.5518	135.5375	
23	31.5457	135.5229	
24	31.5460	135.5280	350.2174
25	31.5465	135.5272	350.1080
26	31.5462	135.5270	350.0897
27	31.5463	135.5272	350.1006
28	31.5463	135.5271	350.0982
29	31.5463	135.5271	350.0986
30	31.5463	135.5271	350.0986

$$|\omega_i^{(n)} - \omega_i^{(n-1)}| < \varepsilon. \quad (51)$$

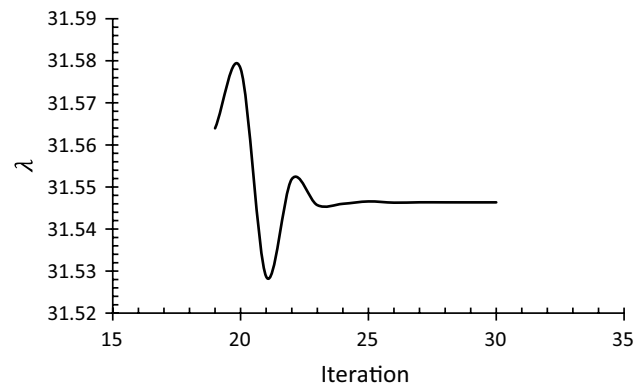
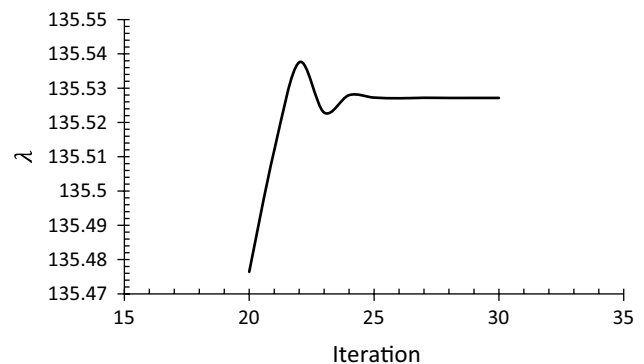
In this study, $\varepsilon = 0.0001$ is considered in the procedure of finding eigenvalues which results in four-digit precision in the estimated eigenvalues. Further a Matlab program has been developed according to the DTM rule as stated before, to find eigenvalues.

3 Results and discussion

In the present section, a numerical testing of the procedure as well as parametric studies is performed to establish the validity and usefulness of the DTM approach and the influence of different beam parameters such as constituent volume fractions, slenderness ratios, rotational speed, and hub radius on the natural frequencies and mode shapes of the rotating beam. The material properties of the power-law FG constituents are presented in Table 3. Relations described in Eq. (52) are performed to calculate the non-dimensional natural frequencies

$$\lambda = \frac{\omega L^2}{h} \sqrt{\frac{\rho_m}{E_m}}. \quad (52)$$

Table 4 shows the convergence study of the DTM method for first three frequencies. It is found that in the

**Fig. 2** Convergence study of first frequency, $L/h = 20$, $P = 2$ **Fig. 3** Convergence study of second frequency, $L/h = 20$, $P = 2$

DTM method after a certain number of iterations, the eigenvalues converged to a value with good precision, so the number of iterations is important in DTM method convergence. From the results of Table 4, high convergence rate of the method may be easily observed. For better observations, Figs. 2 and 3 show the convergence trend of DTM for the first and second frequencies. As seen in Fig. 2, the first natural frequency converged after 27 iterations with four-digit precision, while according to Fig. 3 the second natural frequency converged after 29 iterations.

After looking into the satisfactory results for the convergence of frequencies, to demonstrate the correctness of the present study, the results for FG rotating beam are compared with the results of FG rotating beams presented by Şimşek [9]. Table 5 compares the results of the present study and the results presented by Şimşek [9], which has been obtained by using Lagrange's equations for non-porous FG beam with different slenderness ratios. One may clearly notice here that the fundamental frequency parameters obtained in the present investigation are approximately close enough to the results provided in these studies that are used for comparison and validate the proposed method of solution. Frequency parameters of power-law FG porous

Table 5 Comparison of fundamental frequencies for different power-law indices and slenderness ratio parameter, $\alpha = 0$

L/h	$P = 0.5$		$P = 1$		$P = 10$	
	Present	[9]	Present	[9]	Present	[9]
5	1.6713	1.6744	1.5830	1.5894	1.3039	1.3073
20	1.7204	1.7214	1.6310	1.6357	1.2655	1.2649

Table 6 Variation of the first five natural frequencies of FG rotating beam with power-law exponent, $L/h = 10, \eta = 4$

P	α	λ_1	λ_2	λ_3	λ_4	λ_5
0.5	0	2.7201	11.3777	28.2333	50.4846	76.4422
	0.1	2.7339	11.4364	28.3838	50.7628	76.8761
	0.2	2.7507	11.5084	28.568	51.1033	77.4070
1	0	2.5842	10.7953	26.7389	47.7180	72.1224
	0.1	2.5842	10.7953	26.7389	47.7180	72.1224
	0.2	2.5842	10.7953	26.7389	47.7180	72.1224
2	0	2.4774	10.3131	25.4195	45.1276	67.8858
	0.1	2.4643	10.2534	25.2544	44.801	67.3493
	0.2	2.4475	10.1767	25.0418	44.3795	66.6561
5	0	2.3169	9.5960	23.4847	41.3854	61.8485
	0.1	2.2799	9.4252	23.0080	40.4400	60.2980
	0.2	2.2309	9.1959	22.3599	39.1445	58.1657
10	0	2.1385	8.8510	21.6405	38.0975	56.8844
	0.1	2.0712	8.5500	20.8297	36.5367	54.3809
	0.2	1.9793	8.1319	19.6856	34.3109	50.7904
Metal	0	1.6105	6.7261	16.6539	29.7092	44.8877
	0.1	1.4212	5.9346	14.6920	26.2046	39.5862
	0.2	1.1216	4.6822	11.5862	20.6551	31.1889

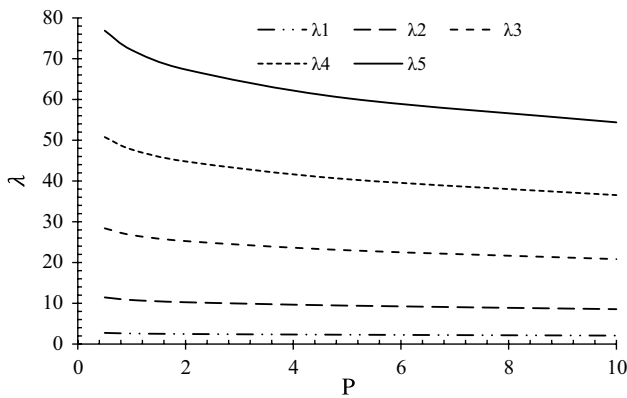


Fig. 4 Effect of power-law indices on the first five natural frequencies of FG rotating beam, $L/h = 10, \eta = 4, \alpha = 0.1$

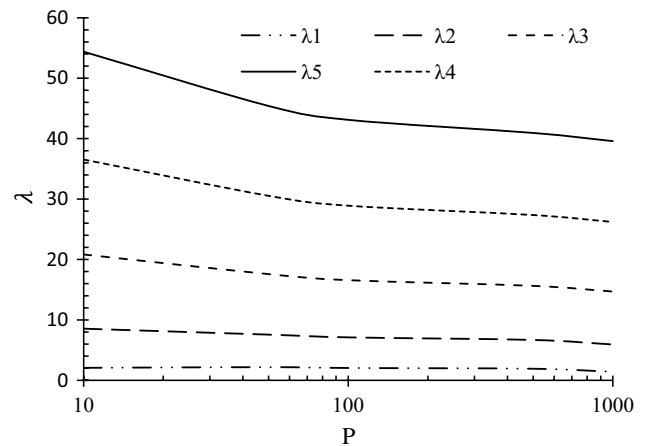


Fig. 5 Effect of power-law indices on the first five natural frequencies of FG rotating beam, $L/h = 10, \eta = 4, \alpha = 0.1$

beam affected by various porosity parameters are studied in Table 6. Inspection of this table reveals that an increase in the value of the power-law exponent leads to a decrease in the fundamental frequencies. The lowest frequency values are obtained for a full metal beam ($P \rightarrow \infty$).

This is due to the fact that an increase in the value of the power-law exponent results in a decrease in the value

of elasticity modulus and the value of bending rigidity. In other words, the beam becomes flexible as the power-law exponent increases. Therefore, as also known from mechanical vibrations, natural frequencies decrease as the stiffness of a structure decreases. It is also interesting to note that the decrease in the frequency values due to the increase

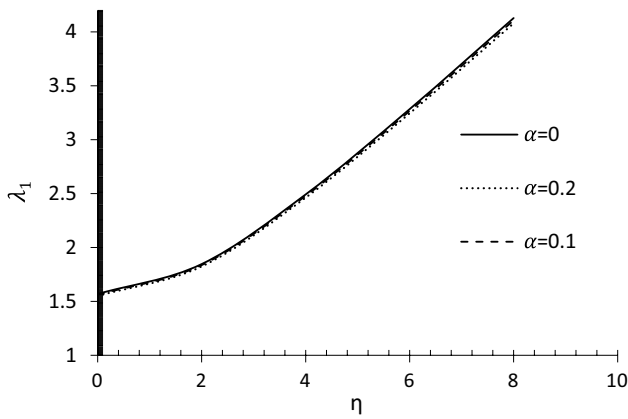


Fig. 6 Effect of hub normal rotational speed and porosity volume fraction on first natural frequency, $L/h = 20, P = 2$

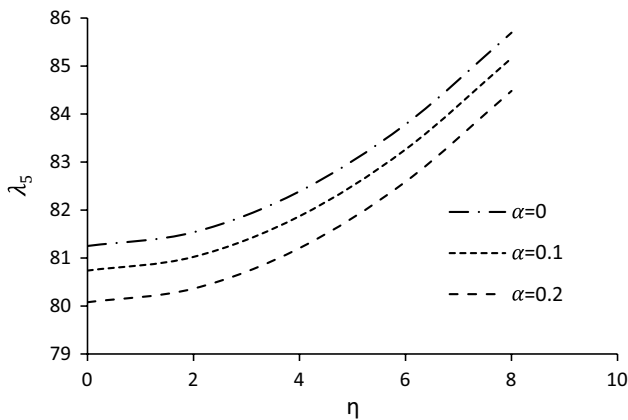


Fig. 7 Effect of hub normal rotational speed and porosity volume fraction on the fifth natural frequency, $L/h = 20, P = 2$

in the power-law exponent is almost the same for higher mode frequencies. It is also observed that an increase in the volume fraction of porosity (α) leads to a slight increase in the fundamental frequencies. Also, the effect of power-law exponent on the first five natural frequencies of the FG rotating beam has been illustrated in Figs. 4 and 5 for two cases of $P < 10$ and $P > 10$, respectively. It is observed that an increase in the value of the power-law exponent leads to a decrease in the fundamental frequencies. Besides, linear reduction occurs when P is increased from 2 to 10. It is shown that the decrease in frequency parameters due to the increase in power-law exponent is also correct for higher mode frequencies.

The other important parameter in vibration behavior of rotating FG beam is its rotational speed parameter. Table 7 presents the variation of the first five natural frequencies of FG porous rotating beam for different rotational speed parameters ($\eta = 0, 2, 4, 6, 8$) with different power-law exponents. It is observed that increasing the rotational speed increases the first five natural frequencies and, as seen in Fig. 7, an ascending pattern is more sensitive for the fifth natural frequency. For instance for FG beam with power-law exponent defined as $P = 2$, increasing normal rotational speed from 2 to 4 leads to 34.9, 7.4, 2.8, 1.5, and 1.04 % increase in the first five natural frequencies, respectively, and on increasing the normal rotational speed from 4 to 8, the first five natural frequencies increase by about 65.6, 23.8, 10.3, 6 and 4 %, respectively.

Also in different rotational speeds when volume fraction of porosities increases, the natural frequencies decrease, while the rate of descent in the first five natural frequencies is not similar. Three lines in Figs. 6 and 7 are plotted for three different values of volume fraction of porosities. Figure 6 and 7 illustrate the effect of rotational speed and

Table 7 The effect of rotational speed parameter on natural frequencies of FG rotating beam with different porosities for the case: $L/h = 20, P = 2$

η	α	λ_1	λ_2	λ_3	λ_4	λ_5
0	0	1.5687	9.7055	26.6413	50.7969	81.2512
	0.1	1.5605	9.6532	26.4913	50.4947	80.7388
	0.2	1.5500	9.5862	26.2988	50.1063	80.0792
2	0	1.8461	9.9657	26.9022	51.0710	81.5374
	0.1	1.8365	9.912	26.7509	50.7676	81.0238
	0.2	1.8242	9.8433	26.5569	50.3777	80.3628
4	0	2.4922	10.7082	27.6684	51.8832	82.3890
	0.1	2.4791	10.6507	27.5134	51.5761	81.8719
	0.2	2.4625	10.5772	27.3145	51.1815	81.2064
6	0	3.2838	11.8415	28.8947	53.2047	83.7855
	0.1	3.2666	11.7782	28.7337	52.8915	83.2626
	0.2	3.2447	11.6972	28.5271	52.4893	82.5898
8	0	4.1288	13.2627	30.5185	54.9922	85.6954
	0.1	4.1072	13.1921	30.3494	54.6708	85.1644
	0.2	4.0796	13.1017	30.1325	54.258	84.4815

Table 8 Variation of the first five natural frequencies of FG rotating beam with L/h ratio for various values of the power-law exponent, $\eta = 2$, $\alpha = 0.1$

P	Mode	$L/h = 5$	$L/h = 10$	$L/h = 20$	$L/h = 30$	$L/h = 50$	$L/h = 100$
5	λ_1	1.6441	1.6885	1.7005	1.7028	1.7039	1.7044
	λ_2	7.5063	8.7328	9.1591	9.2459	9.2914	9.3108
	λ_3	17.1554	22.2583	24.6415	25.1879	25.4844	25.6131
	λ_4	27.8421	39.5906	46.574	48.4012	49.4383	49.8995
	λ_5	38.9996	59.3431	73.993	78.3645	80.9801	82.1788
10	λ_1	1.4924	1.5339	1.5451	1.5472	1.5483	1.5487
	λ_2	6.7833	7.9198	8.3181	8.3994	8.4421	8.4603
	λ_3	15.4561	20.1453	22.3628	22.874	23.1519	23.2726
	λ_4	25.0263	35.7587	42.2283	43.9343	44.9051	45.3376
	λ_5	34.9984	53.5036	67.0202	71.0921	73.5379	74.6613

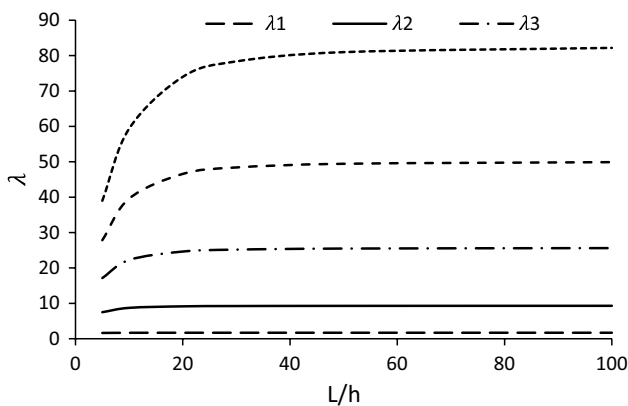


Fig. 8 Effect of slenderness ratio of FG rotating beam on the first five natural frequencies, $\eta = 2$, $P = 5$

Table 9 Effect of hub radius parameter on the first five natural frequencies of an FG rotating beam, $P = 4$, $\eta = 6$, and $\alpha = 0.1$

δ	λ_1	λ_2	λ_3	λ_4	λ_5
0	3.0967	11.1521	27.1408	49.8000	78.1128
0.2	3.3975	11.6286	27.7041	50.4330	78.7990
0.4	3.6729	12.0846	28.2535	51.0559	79.4774
0.6	3.9285	12.5225	28.7901	51.6691	80.1483
0.8	4.1680	12.9442	29.3146	52.2731	80.8119
1	4.394	13.3513	29.8277	52.8681	81.4684

volume fraction of porosity on the first and fifth natural frequencies. In fact, this figure can be regarded as the visual representation of Table 7. It is obvious that the rate of changes in the fifth natural frequency is higher and the volume fraction of porosity has significant effect on higher mode numbers as depicted in Fig. 7.

Also, the effect of slenderness ratio (L/h) on the first five natural frequencies for different power-law exponents is

presented in Table 8. As would be expected, the frequencies are increased when the value of L/h is increased and this effect become less dominant in higher slenderness ratios. Also, the effect of slenderness ratio on the first five natural frequencies of FG rotating beam is plotted in Fig. 8. It can be concluded that by increasing the L/h ratio, the natural frequency parameters increase, while the L/h ratio has more dominant effects on higher mode natural frequencies compared with the lower ones. It is noteworthy that the effect of slenderness ratio on the frequencies is negligible for long FG beams (i.e., $L/h \geq 20$); in other words, the fundamental frequency of the FG rotating beam is saturated after the value of $L/h = 20$.

The next set of results was obtained to demonstrate the effect of hub radius parameter on the non-dimensional natural frequencies of the rotating FG beam. Variations of the first five natural frequencies of rotating FG beam with various hub radius parameters are tabulated in Table 9. Figure 9 illustrates this effect for the first natural frequency when $L/h = 10$, $P = 4$, $\eta = 6$, $\alpha = 0.1$. It is observed that the non-dimensional natural frequencies increase with the increase in hub radius parameter as expected because of the increase in centrifugal stiffening of the beam.

4 Conclusion

In this paper a new semi-analytical model for the vibration analysis of a rotating functionally graded beam made of porous materials was introduced based on Timoshenko beam theory. The differential transform method as an efficient and accurate numerical tool was applied to solve the governing differential equations derived through Hamilton’s principle. The good agreement between the results of this article and those available in literature validated the presented approach. After demonstrating the fast rate of convergence and accuracy of the approaches, emphasis

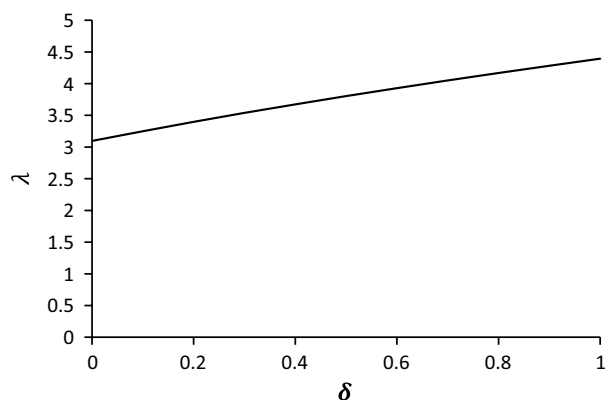


Fig. 9 Effect of hub radius on the first natural frequency of an FG rotating beam, $P = 4$, $\eta = 6$, $\alpha = 0.1$

is placed on investigating the influences of the several parameters such as volume fraction of porosity, mode number, constituent volume fractions, slenderness ratio, rotational speed, and hub radius on the natural frequencies of the rotating porous FG beam. Based on the presented results, one can conclude that rotational speed has a significant influence on natural frequency parameter. Also, it is observed that increasing the porosity and the power-law index has an important effect on the vibration responses of porous FG beam, and the dynamic behavior can be enhanced by selecting appropriate values of the power-law index while the slenderness ratio has negligible effect for long FG beams. Moreover in comparison with other parameters, hub radius has slight effect on natural frequency and increasing hub radius increases natural frequency with low gradient. Numerical results are presented to serve as benchmarks for future analyses of FG porous structures.

References

1. Abdel-Halim Hassan IH (2002) On solving some eigenvalue problems by using a differential transformation. *Appl Math Comput* 127(1):1–22
2. Banerjee JR (2001) Dynamic stiffness formulation and free vibration analysis of centrifugally stiffened Timoshenko beams. *J Sound Vib* 247(1):97–115
3. Ebrahimi F (2013) Analytical investigation on vibrations and dynamic response of functionally graded plate integrated with piezoelectric layers in thermal environment. *Mech Adv Mater Struct* 20(10):854–870
4. Ebrahimi F, Rastgoo A, Atai AA (2009) A theoretical analysis of smart moderately thick shear deformable annular functionally graded plate. *Eur J Mech A Solids* 28(5):962–973
5. Ebrahimi F, Naei MH, Rastgoo A (2009) Geometrically nonlinear vibration analysis of piezoelectrically actuated FGM plate with an initial large deformation. *J Mech Sci Technol* 23(8):2107–2124
6. Ho SH, Chen COK (2006) Free transverse vibration of an axially loaded non-uniform spinning twisted Timoshenko beam using differential transform. *Int J Mech Sci* 48(11):1323–1331
7. Hodges DY, Rutkowski MY (1981) Free-vibration analysis of rotating beams by a variable-order finite-element method. *AIAA J* 19(11):1459–1466
8. Mei C (2008) Application of differential transformation technique to free vibration analysis of a centrifugally stiffened beam. *Comput Struct* 86(11):1280–1284
9. Şimşek M (2010) Fundamental frequency analysis of functionally graded beams by using different higher-order beam theories. *Nucl Eng Des* 240(4):697–705
10. Wattanasakulpong N, Ungbhakorn V (2014) Linear and nonlinear vibration analysis of elastically restrained ends FGM beams with porosities. *Aerosp Sci Technol* 32(1):111–120
11. Wattanasakulpong N, Gangadhara Prusty B, Kelly DW, Hoffman M (2012) Free vibration analysis of layered functionally graded beams with experimental validation. *Mater Des* 36:182–190
12. Zhou JK (1986) *Differential transformation and its applications for electrical circuits*. Huazhong University Press, Wuhan, China